Published in final edited form as:
J Proteome Res. 2013 March 1; 12(3): 1282–1288. doi:10.1021/pr3009397.

Quantitative Proteomic Analysis Revealed *N*′-Nitrosonornicotine-induced Down-regulation of Non-muscle Myosin II and Reduced Cell Migration in Cultured Human Skin Fibroblast Cells

John M. Prins and **Yinsheng Wang***
Department of Chemistry, University of California, Riverside, California 2521-0403

Abstract

The association of tobacco smoke with decreased cell motility and wound healing is well documented; however, the cellular mechanisms and specific toxic tobacco constituents responsible for this effect are not well understood. Tobacco-specific *N*-nitrosamines (TSNAs) are among the most important classes of carcinogens found in tobacco products. The TSNA *N*′-nitrosonornicotine (NNN) is present at relatively high levels in tobacco and its smoke, as well as second- and third-hand smoke. To investigate the cellular pathways that are perturbed upon NNN exposure, we employed a quantitative proteomic approach, utilizing stable isotope labeling by amino acids in cell culture and mass spectrometry, to assess the NNN-induced alteration of protein expression in GM00637 human skin fibroblast cells. With this approach, we were able to quantify 2599 proteins, 191 of which displayed significantly changed expression following NNN exposure. One of the main findings from our proteomic analysis was the down-regulation of six different subunits of myosin, particularly non-muscle myosin II heavy chain, isoforms A, B, and C. In addition, we found the altered expression of several extracellular matrix proteins and proteins involved in cellular adhesion. Together, our quantitative proteomic results suggested that NNN exposure may interfere with fibroblast motility. An *in vitro* scratch wound assay results supported that NNN exposure reduced the ability of dermal fibroblast to migrate into the scratched area. The results from the present study offered novel insights into the cellular mechanisms of NNN toxicity and identified NNN as a specific tobacco constituent that contributes to decreased fibroblast migration.

Keywords

Tobacco-specific N-nitrosamines; NNN; Non-muscle myosin II; mass spectrometry; protein quantitation; cell migration

Introduction

The association of cigarette smoking with inhibited cell migration and wound healing is well recognized and represents a serious health concern associated with tobacco use [1, 2]. Wound healing is a complex process involving the coordination of different cells and proteins that

*To whom correspondence should be addressed: Phone: (951) 827-2700. Fax: (951) 827-4713. yinsheng.wang@ucr.edu.

Supporting Information Available: Western blot results for non-muscle myosin IIa and Iib, scratch assay following a 30-min exposure to 5 μM NNN, LC-MS data for monitoring SILAC labeling efficiency, protein identification and quantification results, and a summary of cellular pathways perturbed in GM00637 cells following NNN exposure. This material is available free of charge via the Internet at http://pubs.acs.org.

respond to injury [3]. Fibroblasts are the most common type of cells of connective tissue and are important for synthesizing and maintaining extracellular matrix proteins. Fibroblasts play a critical role in wound healing and are involved in multiple stages of tissue repair including wound contraction [4]. Earlier studies have demonstrated that cigarette smoke extracts could delay the migration of fibroblast into wounds [5] and inhibit the contraction of wound edges [6]. Although exposure to tobacco smoke was found to be correlated with diminished cell motility and wound healing, the cellular mechanisms and the specific toxic tobacco constituents responsible for this effect are not well understood.

Tobacco-specific *N*-nitrosamines (TSNAs) are considered among the most important classes of carcinogens found in tobacco products and numerous studies have demonstrated that TSNAs are present in substantial quantities in unburned tobacco and its smoke [7]. TSNAs are primarily formed from nicotine during tobacco processing, and TSNAs can also be produced in tobacco smoke residues via surface-mediated reactions between nicotine and ambient nitrous acid [8]. For instance, *N*′-nitrosonornicotine (NNN), a well-known TSNA present at relatively high levels in tobacco and its smoke, is produced through the nitrosation of nornicotine during the curing, aging, processing, and smoking of tobacco, with approximately half of the NNN being formed during burning [9]. NNN has been classified by the International Agency for Research on Cancer (IARC) as a Group 1 carcinogen [7]; it is the most prevalent esophageal carcinogen in cigarette smoke [10]. Although the toxic potential of NNN has been clearly demonstrated in a number of animal models, the overall pathways leading to NNN toxicity has been inadequately investigated.

A major mechanism underlying the toxic effects of NNN exposure is, after cytochrome P450-mediated metabolic activation, its ability to induce DNA adduct formation[7]. Nevertheless, NNN may also exert its cytotoxic effect via altering other cellular pathways. To elucidate the cellular pathways targeted by NNN exposure, we employed a quantitative proteomic technique, based on stable isotope labeling by amino acids in cell culture (SILAC) together with LC-MS/MS, to assess the perturbation of protein expression in GM00637 human skin fibroblast cells. SILAC is a metabolic labeling method, which facilitates the *in vitro* incorporation of stable isotope-labeled amino acids into proteins for mass spectrometry-based protein quantification in the whole proteome [11]. SILAC is dependent upon the incorporation of a given light or heavy form of essential amino acids into proteins, allowing for the generation of two unique cell populations that can be differentiated by LC-MS/MS (Figure 1A). The method facilitates the relative quantification of small changes in protein abundance in cells and allows for the discovery of novel cellular pathways that are altered in response to extracellular stimuli. The results from our quantitative proteomic experiments revealed that 191 proteins were significantly altered in response to NNN treatment. One of the main findings made from our proteomic study was the diminished expression of six different subtypes of myosin and extracellular matrix proteins, including several collagen subtypes and fibronectin, suggesting that NNN exposure may disrupt the migration of dermal fibroblast. To examine the effects of NNN on an *in vitro* cell migration model, we used the scratch wound assay and found that exposing human dermal fibroblast cells to NNN in culture resulted in a reduced ability of these cells to migrate into the scratched area. Thus, our proteomic analysis uncovered a novel mechanism of toxicity for NNN and identified NNN as an important toxic constituent that contributes to compromised wound healing associated with tobacco use.

Materials and Methods

Materials

Heavy lysine and arginine ([$^{13}C_6$,$^{15}N_2$]-L-lysine and [$^{13}C_6$]-L-arginine) were purchased from Cambridge Isotope Laboratories (Andover, MA), and NNN was obtained from Toronto

Research Chemicals Inc. (North York, Ontario, Canada). The polyclonal antibodies against non-muscle myosin IIa and IIb were raised against a synthetic peptide (KLH-coupled) derived from a sequence in the C-terminus of mouse myosin IIa and human myosin IIb (Cell Signaling, Danvers, MA; product #3403 and #3404, respectively). The rabbit anti-actin antibody was purchased from Abcam (Cambridge, MA; product # ab1801).

Cell culture

GM00637 human skin fibroblast cells, kindly provided by Prof. Gerd P. Pfeifer at the City of Hope, were cultured in Iscove's modified Dulbecco's medium (IMDM) supplemented with 10% fetal bovine serum (FBS, Invitrogen, Carlsbad, CA) and penicillin/streptomycin (100 IU/mL). Cells were maintained in a humidified atmosphere with 5% CO_2 at 37°C, and the culture medium was changed at every 2–3 days as needed. For SILAC experiments, custom IMDM medium was prepared without L-lysine or L-arginine according to the American Type Culture Collection (ATCC, Manassas, VA) formulation. The complete light and heavy IMDM media were prepared by the addition of light or heavy lysine and arginine, along with 10% dialyzed FBS, to the above lysine- and arginine-depleted medium. The GM00637 cells were cultured in the heavy lysine- and arginine-containing medium for at least 10 days or 5 cell doublings to achieve complete heavy isotope incorporation (Representative ESI-MS revealing the nearly complete heavy isotope incorporation can be found in Figure S1).

GM00637 cells were cultured to a density of approximately 7.5×10^5 cells/mL. The cells were washed twice with ice-cold phosphate-buffered saline (PBS) to remove the residual FBS, and replaced with FBS-free heavy or light media containing 5 μM NNN or vehicle control (DMSO, final concentration < 0.0025%). In forward SILAC experiments, the cells cultured in light medium were treated with 5 μM NNN for 24 hrs, whereas the cells cultured in heavy medium were untreated and used as control. For reverse SILAC experiments, cells cultured in the heavy medium were treated with NNN and light cells were used as the untreated control (Figure 1A). After 24 hrs, the light and heavy cells were collected by centrifugation at 3,000 g at 4°C, and washed three times with ice-cold PBS. The cell pellets were re-suspended in the CelLytic™ M cell lysis buffer containing a protease inhibitor cocktail (Sigma-Aldrich) and placed on ice for 30 min with vortexing at 10-min intervals. Cell lysates were centrifuged at 12,000 g at 4°C for 30 min, and the resulting supernatants were collected. The protein concentrations of the cell lysates were determined by using Quick Start Bradford Protein Assay kit (Bio-Rad, Hercules, CA). In forward SILAC experiment, the light lysate from NNN-treated cells and the heavy lysate from untreated cells were mixed at 1:1 ratio (100 μg total protein). Proteins were separated by 12% SDS-PAGE with a 4% stacking gel. The gel was stained with Coomassie blue; after destaining, the gel was cut into 20 bands, followed by in-gel reduction with dithiothreitol and alkylated with iodoacetamide. The proteins were digested in-gel with trypsin (Promega, Madison, WI) at an enzyme/protein ratio of 1:100, after which peptides were extracted from gels with 5% acetic acid in H_2O and then with 5% acetic acid in CH_3CN/H_2O (1:1, v/v). The reverse SILAC experiment was performed in a similar fashion except that the heavy lysate of drug-treated cells was mixed with the light lysate from untreated cells. The resulting peptide mixtures were dried and stored at −20°C until further analysis.

LC-MS/MS for protein identification and quantification

The LC-MS/MS experiments were carried out according to our recently described procedures [12]. Briefly, peptide samples were automatically injected and separated by online liquid chromatography on an EASY-nLC, and analyzed on an LTQ Orbitrap Velos mass spectrometer equipped with a nanoelectrospray ionization source (Thermo, San Jose, CA). The separation was conducted by using a home-made trapping column (150 μm×50 mm)

and a separation column (75 μm×120 mm), packed with ReproSil-Pur C18-AQ resin (3 μm in particle size, Dr. Maisch HPLC GmbH, Germany). Peptide samples were initially loaded onto the trapping column with a solvent mixture of 0.1% formic acid in CH_3CN/H_2O (2:98, v/v) at a flow rate of 4.0 μL/min. The peptides were then separated with a 120-min linear gradient of 2–40% acetonitrile in 0.1% formic acid and at a flow rate of 300 nL/min. The LTQ-Orbitrap Velos mass spectrometer was operated in the positive-ion mode, and the spray voltage was 1.8 kV. The data were collected in a data-dependent scan mode where one full-scan MS was followed with twenty MS/MS scans. The full-scan mass spectra (*m/z* 350–2,000) were acquired with a resolution of 60,000 at *m/z* 400 after accumulation to a target value of 500,000. The twenty most abundant ions found in MS at a threshold above 500 counts were selected for fragmentation by collision-induced dissociation at a normalized collision energy of 35%.

Data processing

MaxQuant (Version B.01.03) was employed to extract the MS and MS/MS data [13]. Database search was performed using MaxQuant against the human International Protein Index version 3.68 (87,083 entries) to which contaminants and reverse sequences were added. The search was performed with an initial precursor mass tolerance of 10 ppm and MS/MS tolerance of 0.6 Da. We included cysteine carbamidomethylation and methionine oxidation as fixed and variable modifications, respectively. SILAC quantification setting was adjusted to be doublets, with lysine (+8 Da) and arginine (+6 Da) being selected as heavy labels. Only proteins with at least two peptides being identified by MS/MS were considered as reliably identified. The minimal peptide length was six amino acids, and the maximum number of miss-cleavage for trypsin was set at two per peptide. For peptide and protein identifications, the false discovery rates were set to 1% at both peptide and protein levels [13]. Data normalization is automatically performed by the MaxQuant software. Briefly, MaxQuant assumes that the majority of the proteins in each LC-MS/MS experiment are not significantly altered and the peptide ratios are normalized so that the median of their logarithms is zero, thereby correcting for unequal protein loading [13]. Proteins are quantified based on quantitative information for all peptides identified within a protein. The normalized H/L ratios, significance, and variability (%) were automatically calculated by the MaxQuant program. The quantification was based on three independent SILAC and LC-MS/MS experiments, which included two forward and one reverse SILAC labelings, and the significantly changed proteins discussed below could be quantified in all three sets of SILAC experiments (Figure 1B).

Western Blot

GM00637 cells were cultured in T25 cell culture flask until reaching ~80% confluency as described above. The cells were washed twice with ice-cold phosphate-buffered saline (PBS) to remove the residual FBS, and replaced with FBS-free culture media containing 5 μM NNN or vehicle control (DMSO, final concentration < 0.0025%). The protein concentrations of the cell lysates were determined by using Quick Start Bradford Protein Assay kit (Bio-Rad, Hercules, CA) and 30 μg of protein/sample was used for immunoblotting of non-muscle myosin IIa and IIb. Proteins were separated by SDS-PAGE and transferred to nitrocellulose membranes for immunoblotting. Briefly, proteins were suspended with an equal volume of Laemmli buffer, heated at 95°C for 5 min, loaded, and separated on 12% SDS-PAGE with a 4% stacking gel. Proteins were subsequently transferred to nitrocellulose membrane and blocked in 5% milk in PBS-T buffer (1× phosphate-buffered saline, 0.1% Tween 20, 5% dry milk). Membranes were washed in PBS-T, and incubated overnight at 4°C with primary antibodies (1:1000 for myosin IIa and IIb). Membranes were then washed in PBS-T, incubated with secondary antibody (Cell Signaling, Danvers, MA; product #7074; HRP-conjugated Anti-Rabbit; 1:1000) for 2 hrs, and washed

in PBS-T before imaging with a Typhoon 8600 Fluorescence Imager (Molecular Dynamics/GE Healthcare Biosciences, Pittsburgh, PA, USA). Membranes were re-probed with anti-actin antibody (1:10,000) to confirm equal protein loading. Band pixel intensity was measured using ImageQuant. Band intensities for myosin IIa and IIb from control and NNN-treated groups were normalized to that of actin.

Scratch wound assays

In vitro scratch assays were performed as previously described with minor modifications [14]. Each well of a 6-well tissue culture plates was seeded with GM00637 cells to a final density of 500,000 cells per well and maintained at 37°C in the presence of 5% CO_2 for 24 hrs to permit cell adhesion and formation of a confluent monolayer. After 24 hrs, the medium was removed and replaced with fresh control medium or medium containing 5 μM NNN and treated for another 30 min or 24 hrs. These confluent monolayers were then scored with a sterile pipette tip to leave a scratch of approximately 0.6–0.7 mm in width. Culture medium was then immediately removed (along with any dislodged cells), and the cells were subsequently cultured in fresh culture medium with or without NNN. Images were collected at 12, 24 and 36 hr time points and all scratch assays were performed in six replicates. To monitor the inhibitory effects of NNN on the migration of GM00637 cells, the percentage of the scratch area closed (% area closed) was determined for each treatment group. Images were converted to 8-bit grey scale, and the scratch area and perimeter measurements for each time point were made using Image J 1.46r program (NIH. http://rsb.info.nih.gov/ij/). The image scale was set to pixels and threshold was set to 0–16 (in a scale of 0–255). The % area closed for each treatment group was determined by comparing the scratch area remaining for each time point to the total scratch area at the 0 hr time point.

Results

Protein identification and quantification

To explore the mechanisms of toxicity of NNN exposure, we employed a quantitative proteomic approach utilizing SILAC coupled with LC-MS/MS to assess the NNN-induced perturbation of protein expression in GM00637 human skin fibroblast cells. To this end, we treated the GM00637 cells with 5 μM NNN for 24 hrs, which was found to induce a less than 5% cell death as determined by MTT assay. It is of note that we employed serum-free medium for all NNN treatment experiments to avoid the potential interactions between NNN and proteins in the FBS. To ensure that the observed changes in protein expression were a result of NNN treatment, we conducted the SILAC experiments in triplicate, incorporating both forward and reverse SILAC labelings (Figure 1A, see also Materials and Methods). Figure 2 displays the quantification of the peptide ALEEAMEQK from the myosin heavy chain, non-muscle IIa, which clearly reveals the NNN-induced down-regulation of this protein in both forward and reverse SILAC experiments (Figure 2A and 2B). The sequence for the light- and heavy-labeled peptide was confirmed by MS/MS analysis (Figure 2C and 2D).

Our proteomic analysis allowed for the identification and quantification of 4228 and 3653 proteins, respectively. A total of 2599 proteins could be quantified in both forward and reverse SILAC labeling experiments (Figure 1B), and the detailed quantification results for these proteins are summarized in Table S1. The majority of the quantified proteins were not altered by NNN treatment with an average ratio and average relative standard deviation (RSD) of ratios for all quantified proteins being ~1.0 and 20%, respectively. Thus, a ratio of >1.5 or <0.67 was selected as threshold for screening the significantly changed proteins [1516]. Among the quantified proteins, 191 exhibit significant changes upon NNN treatment (the ratio of protein expression level in treated over untreated cells was greater than 1.5 or less

than 0.67), with 67 and 124 being up- and down-regulated, respectively. The quantification results for all the significantly changed proteins measured in forward and reverse SILAC experiments are summarized in Table S2.

Pathways perturbed by NNN treatment

Analysis of the protein quantification results using GenMAPP/MAPPFinder revealed the perturbation of multiple cellular pathways in GM00637 cells following NNN treatment (Table S3). Proteins with greater than a 1.5-fold change in expression following NNN treatment were included for the analysis, and those pathways with z-scores > 2.0 were considered significant. The primary pathways that were altered upon NNN exposure included myosin (GO, z-score = 5.42), extracellular matrix (GO, z-score = 5.33), and cell adhesion (GO, z-score = 5.12).

Myosins are down-regulated upon NNN treatment

One of the major findings from our quantitative proteomic results was the down- regulation of 6 different subtypes of myosin proteins, including non-muscle myosin heavy chain II subtypes-A, B, and C. Non-muscle myosin II are major cytoskeletal proteins that interact with actin to contribute to various cellular processes including cell migration, cytokinesis, and cell adhesion [17, 18]. The results from our proteomic analysis indicated that, following a 24-hr exposure to 5 μM NNN, non-muscle myosin heavy chain II subtypes-A, B, and C were decreased to 55%, 49%, and 57% relative to mock-treated cells, respectively (Table 1). The down-regulation of myosin IIa and IIb was further confirmed by Western blot analysis (Figure S2). Additionally, our quantitative proteomic experiment demonstrated that NNN treatment resulted in the down-regulation of myosin regulatory light chain 9, myosin regulatory light chain 3, and cardiac myosin light chain 1, which were reduced to levels that are 43%, 56%, and 46% with respect to control cells, respectively (Table 1).

Altered expression of extracellular matrix proteins

Apart from the observed down-regulation of the myosin proteins, our quantitative proteomic analysis demonstrated that NNN treatment also resulted in the perturbation of extracellular matrix proteins which play important roles in cell migration and adhesion [19]. For instance, several different collagen subtypes; alpha 1 & 2 type-I and alpha 1 & 3 type-VI were all down-regulated by 3–4 fold. In contrast, collagen alpha 1 type-VII was increased by 2.25 fold. Collagen plays an important role in cell migration [20]; therefore, altered expression levels of the collagen proteins may interfere with efficient fibroblast motility. In addition, the expression levels of other extracellular matrix proteins that play key roles in cell migration, including laminin beta-2 subunit (a.k.a. laminin B1s), fibronectin, and protein-glutamine gamma-glutamyltransferase 2 [21, 22], were significantly down-regulated, with the ratios of expression levels for treated over untreated cells being 0.52, 0.59, and 0.66, respectively.

Altered expression of proteins involved with cellular adhesion

Analysis of the protein quantification results using GenMAPP identified cellular adhesion as one of the major biological pathways significantly altered as a result of NNN treatment. Cell adhesion is the binding of a cell to a surface, extracellular matrix or another cell using cell adhesion molecules and plays a central role in cell migration [19]. Altered expression of proteins associated with the cellular adhesion pathway identified by GenMapp, which included the extracellular matrix proteins collagen alpha 1 & 3 type-VI, collagen alpha 1 type-VII, fibronectin, and laminin B1s chain, as described above. Additionally, we identified several other cell adhesion proteins that displayed significantly altered expression levels as a result of NNN treatment. These include CD9, CD99, endoglin, symplekin, protein tyrosine

kinase 7, neuronal cell adhesion molecule L1 (L1CAM), and immunoglobulin superfamily DCC subclass member 2 (NEO1, Table 1). While most other proteins involved in cell adhesion were down-regulated upon NNN treatment, the CD9 molecule and symplekin were found to be increased by 1.58 and 1.78 folds, respectively. CD9 is a cell surface protein that has been implicated in a number of cellular processes including cutaneous wound healing [23]; CD9 was down-regulated in migrating epidermis, and re-elevated to basal level when re-epithelialization was completed, supporting that low level of CD9 is required for normal wound healing [23]. Although its function is not fully understood, CD99 is thought to be involved in a number of cellular events such as cell-cell adhesion and maintenance of cellular morphology, and altered expression levels of CD99 have been found in several types of cancer [24]. We found that CD99 was decreased by 45% (i.e., ratio of treated/untreated cells being 0.55) as a result of NNN exposure. Protein tyrosine kinase 7 is a transmembrane receptor that functions as a molecular switch in the Wnt signaling pathway and thought to be required for epidermal wound repair [25]. We found that the expression of protein tyrosine kinase 7 was decreased in NNN-treated cells to a level that is 61% of the control cells. Endoglin, a membrane glycoprotein located on cell surfaces being part of the TGF -β receptor complex, is involved in the cytoskeleton organization and affects cell morphology and migration [26]; its expression was again decreased substantially (a ratio of 0.62 for treated/untreated cells). L1CAM and NEO1, which belong to the immunoglobulin super-family and play important roles in cell-cell adhesion [27, 28], were down-regulated to levels that are 65% and 28% of those of control cells, respectively.

NNN treatment led to reduced migration of skin fibroblast cells

An overarching feature of our proteomic results was that NNN treatment appeared to primarily affect the expression levels of myosin, extracellular matrix, and cell adhesion proteins, suggesting that NNN exposure may impact cell motility and migration in GM00637 cells. To test this, we investigated the inhibitory effects of NNN on the migration of GM00637 cells by using the scratch wound assay [14]. In this assay, a confluent monolayer of GM00637 dermal fibroblasts was scored with a sterile pipette tip and the cells were monitored over time as they repopulated the scratch area [14]. We found that exposure to 5 μM NNN for 24 hrs lead to a significant reduction in the ability of GM00637 cells to migrate into the scratched area (Figure 3); exposure to 5 μM NNN for 30 min, however, failed to reduce the ability of GM00637 cells to migrate into the scratch area (Figure S3).

Discussion

Tobacco smoke contains a complex mixture of toxic constituents. Although there is a clear association between tobacco smoke and decreases in cell motility and wound healing [1, 2, 5], the cellular mechanisms and specific toxic tobacco constituents responsible for this effect are not well understood. NNN is a well-known tobacco carcinogen found at relatively high levels in tobacco and its smoke [7, 29]. NNN constitutes the most prevalent esophageal carcinogen present in cigarette smoke [9], though the underlying mechanisms contributing to its carcinogenic effect have not been extensively investigated.

We conducted a SILAC-based quantitative proteomic study to assess the effects of NNN exposure on protein expression levels in human skin fibroblast cells. One of the main findings from our proteomic analysis was the down-regulation of six different subunits of cellular myosin, particularly non-muscle myosin II heavy chain isoforms A, B, and C. Non-muscle myosin II is an actin-binding protein that has actin cross-linking and contractile properties and is central in the control of cell adhesion, cell migration and tissue architecture [18]. In addition to the three heavy chain isoforms of non-muscle myosin, we found that two 20 kDa regulatory light chains were down-regulated upon NNN treatment (myosin regulatory light chain 9 and myosin regulatory light chain MRCL3 variant; Table

1). These results suggest that NNN exposure induced a decrease in non-muscle myosin II, which may interfere with fibroblast motility.

Cellular migration is an intricate process involving hundreds of proteins that power and regulate cell motility, where cellular adhesion and the extracellular matrix are essential [30]. In this vein, cells initiate migration by adhering to the extracellular matrix which allows for the generation of forces that move the cells forward, followed by disassembly of adhesions at the rear of the cell [30]. Aside from down-regulation of non-muscle myosin II, we found that NNN treatment resulted in the altered expression of several extracellular matrix proteins including collagen type VI and fibronectin (Table 1). Interestingly, an earlier report by Oono et al. [31] showed an increase in collagen type VI gene expression during the early stages of wound healing. In addition, cigarette smoking has been shown to result in a decrease in collagen production, which may be associated with diminished wound healing [32]. Thus, the NNN-induced decrease in collagen VI may contribute to the observed decrease in migration of GM00637 cells following NNN exposure. Additionally, the expression levels for many proteins involved in cellular adhesion were found to be altered in response to NNN treatment, including the CD9 and CD99, which have been shown to be involved in cutaneous wound healing and cell-cell adhesions, respectively [2324]. Taken together, the results from our quantitative proteomic experiments suggest that NNN exposure may disrupt fibroblast migration. By using a scratch wound assay, we indeed found that exposure to 5 μM NNN for 24 hrs dramatically reduced the ability of GM00637 cells to migrate into scratched area, further supporting the results from the proteomic experiments. Together, results from this study offered novel insights into the cellular mechanisms of NNN toxicity and identified NNN as an important toxic tobacco constituent that contributes to the decreases in cell motility and wound healing associated with tobacco smoke exposure. Future experiments are needed for understanding the upstream cellular events leading to the NNN-induced down-regulation of proteins involved in cell motility and wound healing.

Supplementary Material

Refer to Web version on PubMed Central for supplementary material.

Acknowledgments

This research was supported by the National Institutes of Health (R01 DK082779), and John M. Prins was supported by an NRSA T32 institutional training grant (T32 ES018827) and a Postdoctoral Fellowship Award from the California Tobacco-Related Disease Research Program (21FT-0086).

Abbreviations

TSNA	Tobacco specific *N*-nitrosamine
NNN	*N*′-nitrosonornicotine
SILAC	stable isotope labeling by amino acids in cell culture
MS	mass spectrometry
IMDM	Iscove's modified Dulbecco's medium
FBS	fetal bovine serum
SDS-PAGE	sodium dodecyl sulfate-polyacrylamide gel electrophoresis

References

1. Silverstein P. Smoking and wound healing. Am J Med. 1992; 93:22S–24S. [PubMed: 1323208]

2. Metelitsa AI, Lauzon GJ. Tobacco and the skin. Clin Dermatol. 2010; 28:384–90. [PubMed: 20620754]
3. Schultz GS, Wysocki A. Interactions between extracellular matrix and growth factors in wound healing. Wound Repair Regen. 2009; 17:153–62. [PubMed: 19320882]
4. Gabbiani G. The myofibroblast in wound healing and fibrocontractive diseases. J Pathol. 2003; 200:500–3. [PubMed: 12845617]
5. Wong LS, Green HM, Feugate JE, Yadav M, Nothnagel EA, Martins-Green M. Effects of "second-hand" smoke on structure and function of fibroblasts, cells that are critical for tissue repair and remodeling. BMC Cell Biol. 2004; 5:13. [PubMed: 15066202]
6. Carnevali S, Nakamura Y, Mio T, Liu X, Takigawa K, Romberger DJ, Spurzem JR, Rennard SI. Cigarette smoke extract inhibits fibroblast-mediated collagen gel contraction. Am J Physiol. 1998; 274:L591–8. [PubMed: 9575878]
7. Hecht SS. Biochemistry, biology, and carcinogenicity of tobacco-specific N-nitrosamines. Chem Res Toxicol. 1998; 11:559–603. [PubMed: 9625726]
8. Sleiman M, Gundel LA, Pankow JF, Jacob P 3rd, Singer BC, Destaillats H. Formation of carcinogens indoors by surface-mediated reactions of nicotine with nitrous acid, leading to potential thirdhand smoke hazards. Proc Natl Acad Sci USA. 2010; 107:6576–81. [PubMed: 20142504]
9. Stepanov I, Knezevich A, Zhang L, Watson CH, Hatsukami DK, Hecht SS. Carcinogenic tobacco-specific N-nitrosamines in US cigarettes: three decades of remarkable neglect by the tobacco industry. Tob Control. 2012; 21:44–8. [PubMed: 21602537]
10. Yuan JM, Knezevich AD, Wang R, Gao YT, Hecht SS, Stepanov I. Urinary levels of the tobacco-specific carcinogen N′-nitrosonornicotine and its glucuronide are strongly associated with esophageal cancer risk in smokers. Carcinogenesis. 2011; 32:1366–71. [PubMed: 21734256]
11. Ong SE, Blagoev B, Kratchmarova I, Kristensen DB, Steen H, Pandey A, Mann M. Stable isotope labeling by amino acids in cell culture, SILAC, as a simple and accurate approach to expression proteomics. Mol Cell Proteomics. 2002; 1:376–386. [PubMed: 12118079]
12. Zhang F, Dai X, Wang Y. 5-Aza-2′-deoxycytidine induced growth inhibition of leukemia cells through modulating endogenous cholesterol biosynthesis. Mol Cell Proteomics. 2012; 11:M111 016915.
13. Cox J, Mann M. MaxQuant enables high peptide identification rates, individualized p.p.b.-range mass accuracies and proteome-wide protein quantification. Nat Biotechnol. 2008; 26:1367–72. [PubMed: 19029910]
14. Liang CC, Park AY, Guan JL. In vitro scratch assay: a convenient and inexpensive method for analysis of cell migration in vitro. Nat Protoc. 2007; 2:329–33. [PubMed: 17406593]
15. Dong X, Xiao Y, Jiang X, Wang Y. Quantitative proteomic analysis revealed lovastatin-induced perturbation of cellular pathways in HL-60 cells. J Proteome Res. 2011; 10:5463–71. [PubMed: 21967149]
16. Xiong L, Wang Y. Quantitative proteomic analysis reveals the perturbation of multiple cellular pathways in HL-60 cells induced by arsenite treatment. J Proteome Res. 2010; 9:1129–37. [PubMed: 20050688]
17. Matsumura F. Regulation of myosin II during cytokinesis in higher eukaryotes. Trends Cell Biol. 2005; 15:371–7. [PubMed: 15935670]
18. Vicente-Manzanares M, Ma X, Adelstein RS, Horwitz AR. Non-muscle myosin II takes centre stage in cell adhesion and migration. Nat Rev Mol Cell Biol. 2009; 10:778–90. [PubMed: 19851336]
19. Berrier AL, Yamada KM. Cell-matrix adhesion. J Cell Physiol. 2007; 213:565–73. [PubMed: 17680633]
20. Rhee S. Fibroblasts in three dimensional matrices: cell migration and matrix remodeling. Exp Mol Med. 2009; 41:858–65. [PubMed: 19745603]
21. Hamill KJ, Hopkinson SB, Hoover P, Todorovic V, Green KJ, Jones JC. Fibronectin expression determines skin cell motile behavior. J Invest Dermatol. 2012; 132:448–57. [PubMed: 21956124]
22. Antonyak MA, Li B, Regan AD, Feng Q, Dusaban SS, Cerione RA. Tissue transglutaminase is an essential participant in the epidermal growth factor-stimulated signaling pathway leading to cancer cell migration and invasion. J Biol Chem. 2009; 284:17914–25. [PubMed: 19403524]

23. Zhang J, Dong J, Gu H, Yu S, Zhang X, Gou Y, Xu W, Burd A, Huang L, Miyado K, Huang Y, Chan HC. CD9 is critical for cutaneous wound healing through JNK signaling. J Invest Dermatol. 2011; 132:226–36. [PubMed: 21881583]
24. Lee JH, Kim SH, Wang LH, Choi YL, Kim YC, Kim JH, Park TS, Hong YC, Shin YK. Clinical significance of CD99 down-regulation in gastric adenocarcinoma. Clin Cancer Res. 2007; 13:2584–91. [PubMed: 17473187]
25. Peradziryi H, Tolwinski NS, Borchers A. The many roles of PTK7: a versatile regulator of cell-cell communication. Arch Biochem Biophys. 2012; 524:71–6. [PubMed: 22230326]
26. Sanz-Rodriguez F, Guerrero-Esteo M, Botella LM, Banville D, Vary CP, Bernabeu C. Endoglin regulates cytoskeletal organization through binding to ZRP-1, a member of the Lim family of proteins. J Biol Chem. 2004; 279:32858–68. [PubMed: 15148318]
27. Bae GU, Yang YJ, Jiang G, Hong M, Lee HJ, Tessier-Lavigne M, Kang JS, Krauss RS. Neogenin regulates skeletal myofiber size and focal adhesion kinase and extracellular signal-regulated kinase activities in vivo and in vitro. Mol Biol Cell. 2009; 20:4920–31. [PubMed: 19812254]
28. Wai Wong C, Dye DE, Coombe DR. The role of immunoglobulin superfamily cell adhesion molecules in cancer metastasis. Int J Cell Biol. 2012 Article ID 340296.
29. Hecht SS. Progress and challenges in selected areas of tobacco carcinogenesis. Chem Res Toxicol. 2008; 21:160–71. [PubMed: 18052103]
30. Ridley AJ, Schwartz MA, Burridge K, Firtel RA, Ginsberg MH, Borisy G, Parsons JT, Horwitz AR. Cell migration: integrating signals from front to back. Science. 2003; 302:1704–9. [PubMed: 14657486]
31. Oono T, Specks U, Eckes B, Majewski S, Hunzelmann N, Timpl R, Krieg T. Expression of type VI collagen mRNA during wound healing. J Invest Dermatol. 1993; 100:329–34. [PubMed: 8440917]
32. Jorgensen LN, Kallehave F, Christensen E, Siana JE, Gottrup F. Less collagen production in smokers. Surgery. 1998; 123:450–5. [PubMed: 9551072]

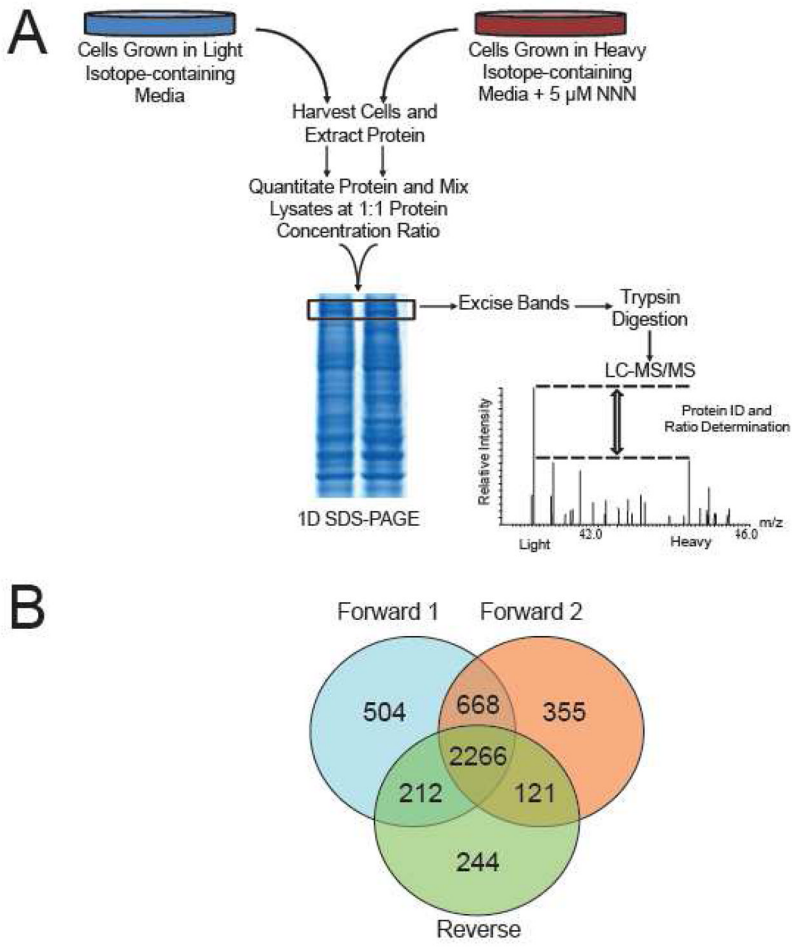

Figure 1.

SILAC-based quantitative proteomics. (A) Flowchart of reverse SILAC coupled with LC-MS/MS for the comparative analysis of protein expression in GM00637 cells following NNN treatment. In forward SILAC experiments, light Lys- and Arg-labeled cells were treated with 5 μM NNN, whereas the heavy Lys- and Arg-labeled cells were used as vehicle control. (B) A Venn diagram summarizing the number of proteins quantified from three independent SILAC (two forward and one reverse) experiments.

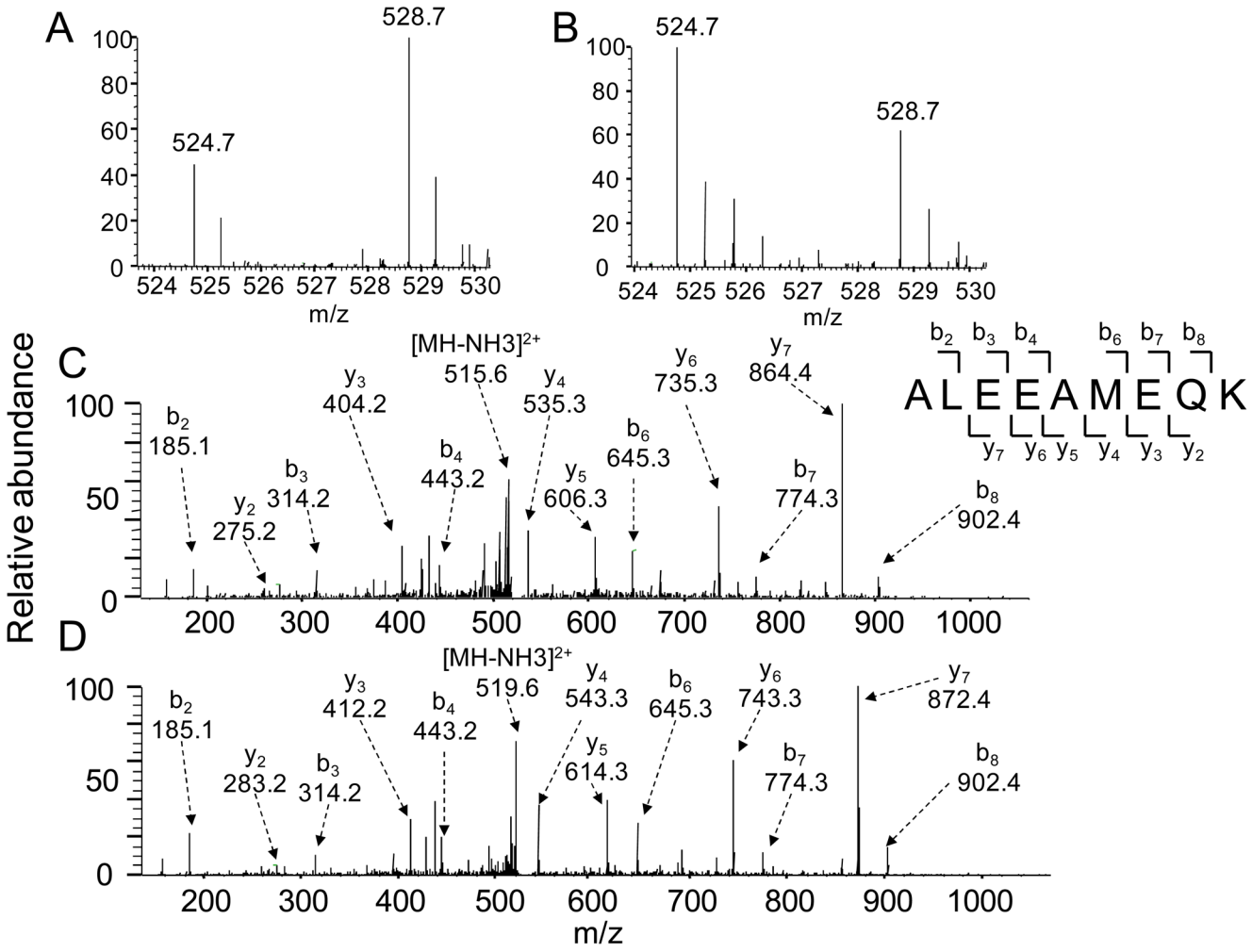

Figure 2.

Representative LC-MS/MS data revealed the NNN-induced down-regulation of the peptide ALEEAMEQK from the non-muscle myosin heavy chain IIa. Shown are the mass spectra for the $[M + 2H]^{2+}$ ions of the peptide ALEEAMEQK from the forward (A) and reverse (B) SILAC samples. The sequence for both the light- and heavy-labeled peptide was confirmed by MS/MS analysis, depicted in (C) and (D), respectively.

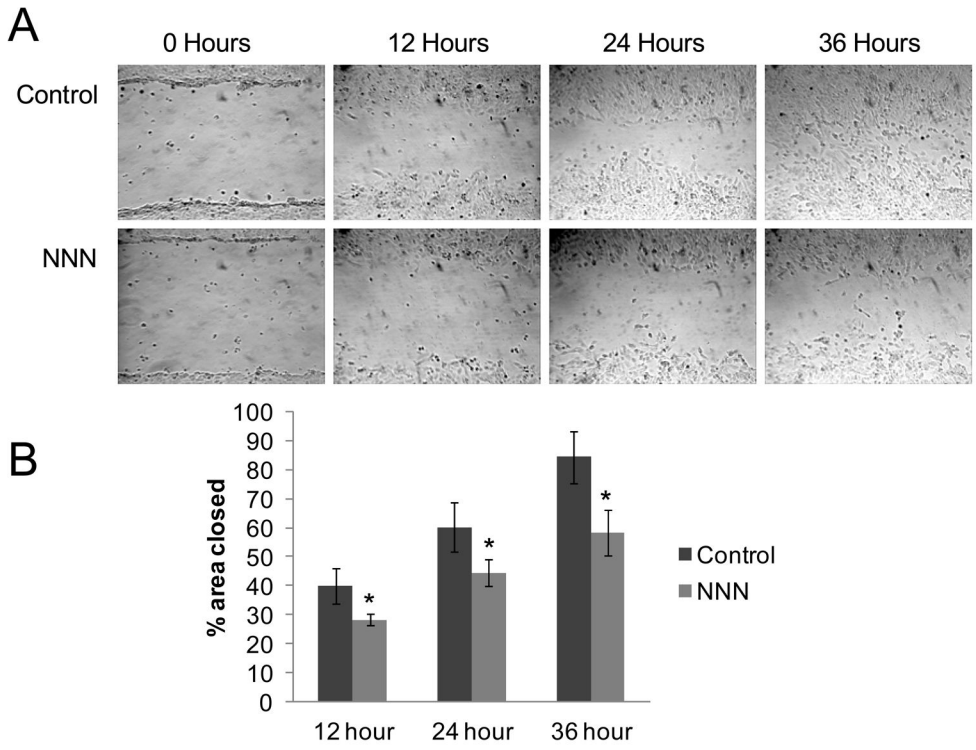

Figure 3.

In vitro scratch assay for GM00637 cells following treatment with 5 μM NNN for 24 hrs. (A) Exposure to 5 μM NNN for 24 hrs dramatically reduced the ability of GM00637 cells to migrate into scratch area. (B) The percentage of the scratch area closed relative to the 0 hr time point. Data represent the mean ± standard deviation. '*', $p < 0.05$, student-t test (n=6).

Table 1

Significantly altered proteins involved in cellular migration and adhesion, with IPI numbers, protein names, average ratios and standard deviation listed. A complete list of all proteins with > ±1.5 fold changes is shown in Table S2.

IPI Number	Protein Name	Average Ratio (Treated/Untreated)
	A. Myosin	
IPI00019502	Myosin heavy chain, non-muscle IIa	0.55 ± 0.12
IPI00790503	Myosin heavy chain, non-muscle IIb	0.49 ± 0.07
IPI00926581	Myosin heavy chain, non-muscle IIc	0.57 ± 0.16
IPI00220278	Myosin regulatory light chain 9 (20 kDa)	0.43 ± 0.10
IPI00604523	Myosin regulatory light chain MRCL3 variant (20 kDa)	0.56 ± 0.10
IPI00243742	Cardiac myosin light chain 1	0.46 ± 0.09
	B. Extracellular Matrix	
IPI00294578	Protein-glutamine gamma-glutamyltransferase 2	0.66 ± 0.16
IPI00855785	Fibronectin	0.59 ± 0.24
IPI00296922	Laminin B1s chain	0.52 ± 0.09
IPI00297646	Alpha-1 type I collagen	0.25 ± 0.03
IPI00304962	Alpha-2 type I collagen	0.30 ± 0.07
IPI00291136	Collagen alpha-1(VI) chain	0.25 ± 0.15
IPI00025418	Collagen alpha-1(VII) chain	2.25 ± 0.58
IPI00022200	Collagen alpha-3(VI) chain	0.27 ± 0.05
	C. Cell Adhesion	
IPI00291136	Collagen alpha-1(VI) chain	0.25 ± 0.15
IPI00025418	Collagen alpha-1(VII) chain	2.25 ± 0.58
IPI00022200	Collagen alpha-3(VI) chain	0.27 ± 0.05
IPI00215997	CD9 molecule	1.58 ± 0.28
IPI00253036	CD99 molecule	0.55 ± 0.13
IPI00855785	Fibronectin	0.59 ± 0.24
IPI00017567	Endoglin	0.62 ± 0.20
IPI00871467	Neural cell adhesion molecule L1 (L1CAM)	0.65 ± 0.19
IPI00296922	Laminin B1s chain	0.52 ± 0.09
IPI00023344	Symplekin	1.78 ± 0.74
IPI00946792	Protein-tyrosine kinase 7	0.61 ± 0.16
IPI00023814	Immunoglobulin superfamily DCC subclass member 2 (Neo1)	0.28 ± 0.11